ASTRONOMY & ASTROPHYSICS
SUPPLEMENT SERIES

Astron. Astrophys. Suppl. Ser. **117,** 189-195 (1996)

An efficient method for dealing with line haze in stellar spectra

Ana M. Larson and Alan W. Irwin

Department of Physics and Astronomy, University of Victoria, Box 3055, MS7700, Victoria, B.C. V8W 3P6 Canada
e-mail: larson@otter.phys.uvic.ca, irwin@otter.phys.uvic.ca

Received June 3; accepted October 7, 1995

Abstract. — When analyzing any wavelength region, stellar spectroscopists must deal with the multitude of weak lines which depress the true continuum and thus form the pseudocontinuum. Calculating the effect of these lines, known collectively as the "line haze," under conventional synthetic spectrum analysis is CPU intensive; an excessive amount of time is often spent calculating the opacity profiles of lines which are too weak to have even a cumulative effect on the line haze. We have developed a method of identifying and eliminating these "ultraweak" lines from synthetic spectrum computations. We treat the line opacity as a perturbation to the continuum opacity and generate tables of equivalent width coefficients which are a function of the model atmosphere, species, excitation potential, and wavelength region. Through interpolation of these tables and knowledge of the gf value for each line, we rapidly and accurately calculate the equivalent width of any line on the linear part of the curve of growth. We then determine the cumulative line blocking as a function of equivalent width. Through the use of this function and a specified line-blocking error, we eliminate from further consideration all lines having little or no effect on the pseudocontinuum. The reduction in the number of lines used in the spectrum synthesis results in a significant savings in computation time. We present the method for 314 000 atomic and molecular lines in the 864−878 nm wavelength region, effective temperatures of 4000−6000 K, $\log g$ of 1.5−4.5 (cgs units), and solar abundances.

Key words: methods: analytical — atomic data — molecular data — stars: atmospheres

1. Introduction

Researchers who synthesize stellar spectra have seen the accuracy of their work increase dramatically with the recent improvements in atomic and molecular line data. Data for approximately 58 million atomic and molecular lines are available from the compilations of Kurucz (1993a, K93a; 1993c, K93c) and 70 million molecular lines from Jørgensen (1994a, J94a). (CN, CH, and TiO data overlap in these compilations.)

We need these extensive line lists not only for the accurate calculation of the strong lines but also for the calculation of the line haze. As is well known, the line haze is formed by the en masse veiling of the continuum by lines which individually are too weak to be visible. However, some lines are too weak to even have a cumulative effect on the line haze. These lines are normally eliminated in synthetic spectrum computations because it takes substantial computer resources to calculate opacity profiles. Typical line rejection criteria, which usually depend on the ratio of line to continuum opacity, introduce the possibility that the computations will cost an excessive amount of computer time (rejection level set too low) or will underestimate the line haze (rejection level set too high).

Send offprint requests to: Ana M. Larson

Our spectrum synthesis code, SSynth, calculates the line haze in a consistent manner; that is, the result has the correct integrated equivalent width over the whole spectral interval. Rather than ignore all lines below some fraction (typically 0.0001) of the continuum opacity, all parts of the Voigt profile (calculated using a modified version of the routine given by Drayson 1976) below this fraction are "smeared" (or averaged) and added to the continuum opacity. This process can be made reasonably efficient since, for weak lines, the program uses mean broadening coefficients and shifts the line centers to the nearest frequency sample points. For each depth and species we can then precompute the Voigt profile as a function of sample point from line center. This minimizes the computer costs for each line. However, if the line list includes large numbers of lines which contribute negligibly to the smeared line opacity and resulting line haze, these costs can rapidly and unjustifiably increase. We call these lines "ultraweak" to distinguish them from the "weak" lines which *do* contribute appreciably to the line haze.

In this paper we describe an algorithm that rapidly eliminates the ultraweak lines from a line list and thus improves the efficiency of the subsequent synthetic spectrum computations without compromising the line haze calculation. This work is part of on-going analyses of the high-quality spectra obtained at the Canada-France-

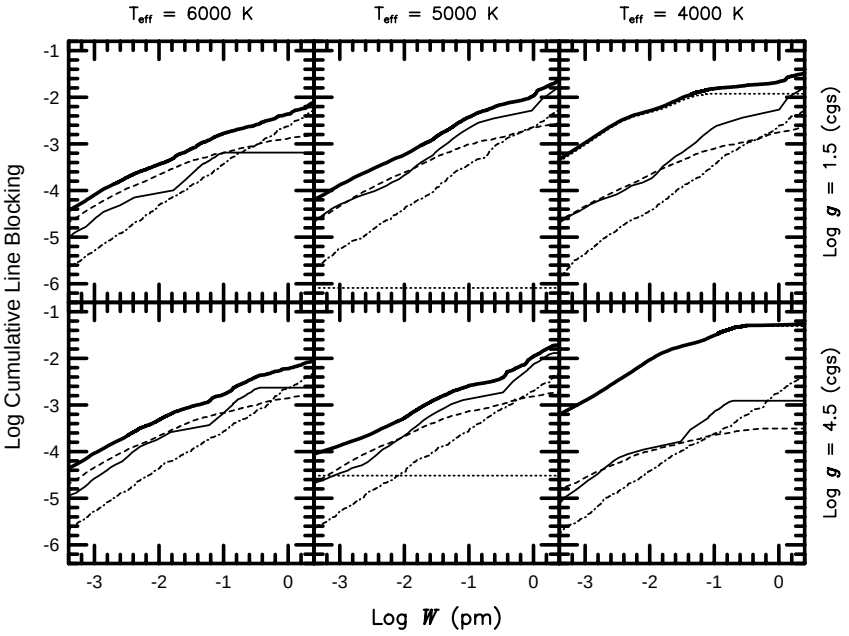

Fig. 1. The cumulative line blocking as a function of equivalent width for lines on the linear part of the curve of growth. The heavy solid line represents all atomic and molecular lines; the dotted line, TiO; the light solid line, CN; the dashed line, atomic lines with predicted energy levels from Kurucz CD-ROM 1 (Kurucz 1993a, referred to as the predicted set in the text); the dot-dashed line, atomic lines with measured energy levels from Kurucz CD-ROM 18 (Kurucz 1993c, referred to as the measured set in the text). Note that the TiO lines provide nearly all of the blocking at $T_{\rm eff} = 4000$ K, $\log g = 4.5$, but are so weak at 6000 K that their total blocking falls below the lower limits plotted

Hawaii Telescope and Dominion Astrophysical Observatory for the precise radial-velocity survey of nearby, solar-type stars (cf. Larson et al. 1993 and references therein). The wavelength region of these spectra is 864−878 nm.

2. Methods

SSynth, our spectrum synthesis code, was initially developed by Irwin (1978). It uses a modified Feautrier-Auer method to solve the equation of transfer (Auer 1976, A76; Mihalas 1978, M78). The program calculates the equation of state using a Newton-Raphson iteration procedure which is equivalent to Helmholtz free-energy minimization. The partition functions are from Irwin (1981, 1987, 1988) and Sauval & Tatum (1984). The relative energy, i.e., ionization potentials, electron affinities, or dissociation or atomization energies, of each species is taken from Moore (1970); Huber & Herzberg (1979); Hotop & Lineberger (1985); Martin et al. (1985 and references therein); Moore (1985 and references therein); Sugar & Corliss (1985); and Irwin (1988).

Our method for eliminating ultraweak lines proceeds in four steps: 1) For a given model atmosphere and wavelength central to the region of interest, we calculate the equivalent width coefficients, $W_0'(\chi)$ [defined by Eq. (3)], for a number of excitation potentials, χ, using a short artificial line list for every species in the line list. We collect these values of $W_0'(\chi)$ in a table as a function of species and χ. 2) We rapidly interpolate this table in χ and combine the derived value of $W_0'(\chi)$ with the gf value of each line to calculate the equivalent widths of all lines in the region [see Eq. (4)]. 3) We calculate the cumulative line blocking as a function of equivalent width [see Eq. (5)]. 4) We use this function to eliminate all lines which contribute negligibly to the line haze (demonstrated in Sect. 3).

We start with the standard definition for the equivalent width of a line

$$W = \int_0^\infty A_\lambda {\rm d}\lambda = \int_0^\infty 1 - \frac{H_\lambda}{H_\lambda^{\rm c}} {\rm d}\lambda \,, \qquad (1)$$

where A_λ is the absorption depth of the line, H_λ is the flux we observe at a given wavelength, λ, and $H_\lambda^{\rm c}$ is the associated continuum flux. For weak lines, $A_\lambda \propto gf$, independent of the details of the depth-dependent opacity profiles. We expand Eq. (1) from $gf = 0$ in a first-order Taylor series to obtain

$$W = gf \int_0^\infty \frac{\partial A_\lambda}{\partial gf} {\rm d}\lambda \,. \qquad (2)$$

For each species, the tabulated equivalent width coefficients are defined by

$$\lim_{gf \to 0} \frac{W}{gf} \equiv W_0'(\chi) \;\; = -\frac{1}{H_\lambda^{\rm c}} \int_0^\infty \frac{\partial H_\lambda}{\partial gf} {\rm d}\lambda \;. \qquad (3)$$

The $W_0'(\chi)$ coefficients could be tabulated as a function of wavelength. However, in our application, we use just the central wavelength; the $W_0'(\chi)$ coefficients are essentially independent of wavelength within the narrow spectral interval 864−878 nm. We assume a boxcar opacity profile and use the chain rule to follow the line opacity perturbation through the equation of transfer. We differentiate the appropriate Feautrier-Auer equations and the line opacity (see Appendix) such that $W = W_0'(\chi)\ gf$ is consistent with the equivalent width SSynth would calculate for isolated weak lines.

Fig. 2. The fraction of lines which would be retained under a 0.1% and a 1% line-blocking error for a range of effective temperatures and $\log g$ values

Once we have tabulated the coefficients, we calculate W_l, the equivalent width of the $l^{\rm th}$ line in the wavelength interval:

$$W_l = W_0'(\chi)_l\ (gf)_l\ . \tag{4}$$

Since this approach is applicable only to weak lines, the calculated equivalent widths of the stronger lines will be overstated. On the other hand, this method extends the calculation of equivalent widths to lines so weak that other methods fail due to numerical significance loss.

We define the cumulative blocking coefficient as

$$\epsilon_\lambda(W) \equiv 1 - \left[\frac{\int H_{\lambda'}{\rm d}\lambda'}{\int H^{\rm c}_{\lambda'}{\rm d}\lambda'}\right] = \frac{\sum_l W_l}{2\,\Delta\lambda}\ , \tag{5}$$

where the right-hand term follows from the assumption that $H^{\rm c}_\lambda$ is constant over the integration range $\lambda \pm \Delta\lambda$. We take the sum over all l such that $W_l \leq W$ to calculate the cumulative line blocking as a function of W (see Fig. 1).

3. Results

We demonstrate our line-elimination method using the 864−878 nm region of late-type stellar spectra. The atmospheres were taken from the grid provided by Kurucz (1993b) for effective temperatures from 4000 to 6000 K, $\log\ g$ from 1.5 to 4.5 (cgs units), solar abundances, and a microturbulence value of 2.0 km s^{-1}. Our line list has approximately 314 000 lines in the 864−878 nm wavelength region. The atomic data and most of the diatomic data in our line list are taken from Kurucz (K93a, K93c). We supplemented Kurucz's CN data with Jørgensen data (J94a, see also Jørgensen & Larsson 1990), which extend to higher J values and nearly to the dissociation limit. The TiO data are from J94a (see also Jørgensen 1994b). Under the conditions examined here, CN and TiO dominate the diatomic line blocking; other diatomics either have no lines in this wavelength region or have a negligible effect. We adopted a CN dissociation energy of 7.9 eV and a TiO dissociation energy of 6.87 eV.

Figure 1 shows the cumulative line blocking as a function of equivalent width for $T_{\rm eff}$ = 6000 K, 5000 K, and 4000 K and $\log g$ = 4.5 and 1.5 (cgs). The heavy, solid line of each graph represents the cumulative line blocking for all of the species which have equivalent widths on the linear part of the curve of growth; the upper limit of the abscissas corresponds to $\log(W/\lambda) \lesssim -5.5$. The lighter lines represent the isolated cumulative line blocking of TiO (dotted), CN (solid) and two atomic line lists (described below).

Some well-known molecular behavior is immediately apparent in Fig. 1. First, the cumulative line blocking for TiO shows a strong temperature dependence; TiO provides nearly all of the cumulative blocking at $T_{\rm eff}$ = 4000 K, but provides essentially no blocking at 6000 K. Second, the TiO blocking decreases with decreasing surface gravity. Since the temperature classification of cool stars is defined by TiO, a giant must be cooler than a dwarf of identical spectral type. Third, the cumulative line blocking for CN increases with decreasing surface gravity at 4000 K, but the effect weakens at 5000 K and slightly reverses at 6000 K. This result agrees qualitatively with the *calculated* results of Bell and Tripicco (1991, Fig. 7) for CN in the blue region of the spectrum. (These authors conclude that an additional mechanism, e.g. nitrogen enhancement and carbon depletion, is required to explain the *observed* CN luminosity effect in the blue for $T_{\rm eff} > 4500$ K.)

The cumulative line-blocking function can also be used for examining the effect of the incompleteness of the line lists. For example, we separated the atomic line data into two sets. The "predicted set" (dashed line of Fig. 1) contains only those lines with predicted energies and wavelengths from the file "lowlines.dat" from CD-ROM 1 (K93a). The "measured set" (dot-dashed line of Fig. 1) contains lines from CD-ROM 18 (K93c), which have measured energies and wavelengths (see Kurucz 1991). While any effective temperature/gravity dependence for the cumulative line blocking of the individual atomic species is masked by the grouping used here, one notes

from Fig. 1 that, although the cumulative line blocking is dominated by the predicted set at small equivalent widths, the total cumulative blocking for the predicted set never exceeds -2.5 dex.

The weakness of the predicted lines is probably the result of a selection effect; Kurucz's predicted lines are unobserved in laboratory spectra and thus tend to be weak not only in laboratory but also stellar spectra. The weakness of the predicted lines for the effective temperatures and gravities considered here suggests the predicted line data may be ignored for our wavelength region. This is a reassuring result; it is precisely for these predicted lines that the model Hamiltonian used in Kurucz's semi-empirical analysis tends to have its largest uncertainties.

Our primary use for the cumulative line-blocking function shown in Fig. 1 is to eliminate the ultraweak lines. We choose an acceptable line-blocking error and retain only those lines whose equivalent widths are greater than the corresponding value. The fraction of lines retained (see Fig. 2) will change as a function of the accuracy desired and as a function of the stellar parameters. For $\log g = 4.5$, one notes, for example, that the fraction of lines retained at a line-blocking error of 0.1% falls from about 0.15 at $T_{\rm eff} = 4000$ K to about 0.001 at $T_{\rm eff} = 6000$ K.

Table 1 shows the execution times, in minutes, for each of the major sections of our synthetic spectrum computations for $T_{\rm eff} = 5000$ K, $\log g = 4.5$, and five separate line lists. All timing was done on a workstation with a capacity of 3.5 mega flops, and the only difference between the computations was the fraction of lines retained in the line lists, as given in the table. For each computation the criterion for the line smearing (or the averaging of the unused portions of each Voigt profile) was set at 0.0001 of the continuum opacity. The equation of transfer was solved with three quadrature angles and 5400 wavelength points, and the continuum scattering was treated as ordinary absorption without stimulated emission (see Appendix).

By separating the execution times attributable to the equation of state (EOS), pre-SSynth (where we process the line lists) and SSynth routines, we highlight those areas where the greatest time savings will occur. We show the calculation of the EOS separately as this calculation is needed only once per model atmosphere. Our pre-SSynth procedure includes the line-elimination method (LEM) described above (except, obviously, where we have included all lines at a line-blocking error of 0.0% for demonstration purposes). It also includes a modified Heapsort (Press et al. 1992) algorithm which sorts the selected line data into manageable wavelength intervals and by species within each wavelength interval. This sorting step greatly facilitates the line opacity and equation of transfer calculations. To make a fair comparison, one should note that the pre-SSynth step would only need to be done once per wavelength region for the 0.0% line-blocking error. However, for non-zero line-blocking errors, the selected line list may be used for a range of stellar models; thus, depending on the tolerable line-blocking error and the range of atmospheric parameters being tested, the pre-SSynth steps may need to be done only infrequently.

The execution time for our SSynth routines, shown in the last line of Table 1, is dominated by the calculation of the line opacity profiles and the solution to the equation of transfer. At the 1% blocking error, the execution time reaches the overhead presented by the solution to the equation of transfer. It is readily apparent from subtracting this overhead that the execution time for the calculation of the line opacity profiles is roughly proportional to the number of lines used. The order-of-magnitude difference between the time for a 0.0% line-blocking error and that for a ≥ 0.1% line-blocking error emphasizes the efficiency of our line-elimination method. In spectral regions having a higher density of lines than the present case, the overhead presented by the solution to the equation of transfer will be a smaller proportion of the execution time and the potential time savings may be greater. The exact savings will depend on the shape of the cumulative line-blocking function. However, our line-elimination method clearly should be considered for all wavelength regions.

Figure 3 superimposes the synthetic spectrum where the line list included all of the lines, 0.0% line-blocking error, and the synthetic spectrum where the line list included -2.55 dex of the lines, 0.1% line-blocking error, over a selected subregion. A line-blocking error of 0.1% was chosen for comparison as this value optimizes the efficiency of our method, as Table 1 shows. The differences between the spectrum computed using all of the lines and the spectrum computed using the abbreviated line list are indiscernible on a normal scale, as shown in the upper plot of Fig. 3. The lower plot shows the spectra on an expanded scale and emphasizes the continuum region. As expected, the errors are of order 0.1% in the pseudocontinuum and less in the lines. From a practical standpoint, if one were using lines having a line depth of 0.05 for abundance analysis one would expect relative errors, in this case, on the order of 2% in the calculated line depth.

4. Summary

Through our treatment of the line haze as a perturbation to the continuum opacity, we have developed an efficient and automatic method of calculating the cumulative line blocking as a function of equivalent width. We use this function along with a specified line-blocking error to eliminate the large number of ultraweak lines, that is, those lines which contribute negligibly to the line haze. This method substantially reduces the line list used in the synthetic spectrum computation without compromising the calculated pseudocontinuum. By reducing the number of lines used, we realize an order-of-magnitude savings in the time needed for computing an individual spectrum. As

Table 1. Approximate execution times for the programs associated with a spectrum synthesis using a workstation having a capacity of 3.5 mega flops for $T_{\rm eff} = 5000$ K $\log g = 4.5$

Line-Blocking Error[a]	**0.0%**	**0.0001%**	**0.01%**	**0.1%**	**1.0%**
Log $N_{\rm r}/N_{\rm t}$[b]	**0.0**	**−0.68**	**−1.96**	**−2.55**	**−3.34**
	Execution Time (minutes)				
EOS[c]	**4.4**	**4.4**	**4.4**	**4.4**	**4.4**
Pre-SSynth:					
LEM[d]	**N/A**	**9.7**	**5.1**	**4.8**	**4.8**
Sort[e]	**26.5**	**4.6**	**0.2**	**<< 1**	**<< 1**
SSynth[f]	**22.6**	**7.0**	**2.7**	**2.2**	**2.0**

[a] Systematic error in pseudocontinuum resulting from the elimination of the ultraweak lines from the line list
[b] $N_{\rm r} \equiv$ number of lines retained, $N_{\rm t} \equiv$ number of lines total
[c] Equation of State (average)
[d] Line-Elimination Method (see text)
[e] Sort uses a modified Heapsort algorithm (Press et al. 1992)
[f] Time is dominated by the calculation of the line opacity profiles and the solution to the equation of transfer

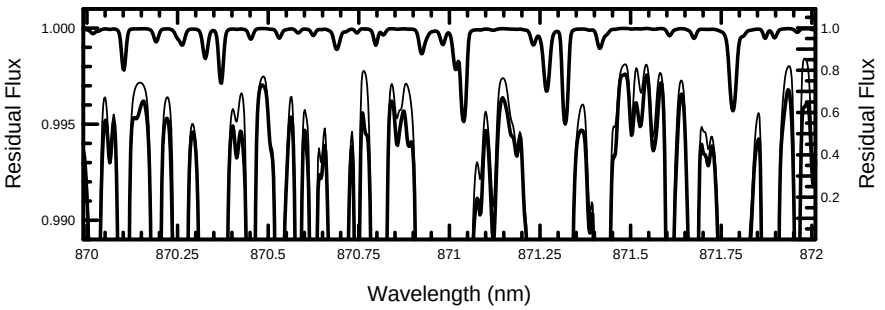

Fig. 3. A portion of the wavelength region for $T_{\rm eff} = 5000$ K, $\log g = 4.5$. The spectrum calculated using all line data is indicated by the heavy line; the spectrum calculated using 0.003 of the line data (selected using a 0.1% line-blocking error), by the light line. The expanded scale shows that the errors in the pseudocontinuum are approximately 0.1%, as expected

a result, we will be able to more efficiently synthesize a greater number of stellar spectra.

While the primary use of the cumulative line-blocking function is to improve the efficiency of our synthetic spectrum computations, there are also a number of secondary uses. For example, we will be able to use these results to further evaluate line list incompleteness and to explore the effect line haze has in stellar population studies. To insure that the cumulative line-blocking function is correct, it is absolutely essential that the calculated line lists are made as complete as possible. However, once that is done, individuals who generate these line lists should be able to use a criterion based on the cumulative line-blocking function to reduce the number of lines they need to distribute for synthetic spectrum purposes.

Acknowledgements. A.M.L. acknowledges support provided by the National Science and Engineering Research Council of Canada through an Operating Grant to D.A. VandenBerg. We thank R.L. Kurucz and U.G. Jørgensen for their fundamental work on the line lists. We also thank U.G. Jørgensen as referee for suggestions which clarified and thus improved the presentation of our method.

A. Appendix

The calculation of the derivatives used in forming the $W_0'(\chi)$ coefficients is entirely consistent with the difference equation method we use to solve the equation of transfer. At the user's discretion, the difference equations can be solved using either the fourth-order Hermitian (A76), the second-order spline collocation (Kunasz & Hummer 1974), or the original second-order Feautrier (M78) method. For simplicity, we demonstrate the derivative calculation using the original Feautrier method, and the reader is referred

to M78 for related equations. The generalization to the other methods is straightforward.

We define $I_d(\mu_i)$ as the monochromatic specific intensity at depth d and angle $\cos^{-1}\mu_i$, for $i = 1, \ldots, N$, where N is the number of discrete angles used. Following M78, Eq. (6-12), we define the symmetric average of the specific intensity:

$$u_d(\mu_i) \equiv \frac{1}{2}[I_d(\mu_i) + I_d(-\mu_i)] \ . \tag{A1}$$

Since all quantities are monochromatic, we have dropped the wavelength subscripts. This leads to the second order equation of transfer for u_d [M78, Eq. (6-17)]:

$$\mu^2 \left[\frac{\partial^2 u_d(\mu_i)}{\partial \tau_d^2}\right] = u_d(\mu_i) - S_d \ . \tag{A2}$$

We assume a simplified source function that allows for continuum scattering:

$$\begin{aligned} S_d &= \alpha_d \int_0^1 u_d(\mu)\,\mathrm{d}\mu + (1-\alpha_d)B(T_d) \\ &= \alpha_d \sum_k w_k u_{d,k} + (1-\alpha_d)B(T_d) \ , \end{aligned} \tag{A3}$$

where w_k is the angle-integration weight for the kth angle point. In this equation, $B(T_d)$ is the monochromatic Planck function evaluated at temperature T_d and α_d is the ratio of the continuum scattering to the total opacity.

To aid in the discretization of the equation of transfer [Eq. (A2)], we define:

$$\Delta\tau_\pm = \frac{1}{2}\left[\left(\frac{\kappa}{\kappa_\mathrm{R}}\right)_d + \left(\frac{\kappa}{\kappa_\mathrm{R}}\right)_{d\pm1}\right] |(\tau_\mathrm{R})_{d\pm1} - (\tau_\mathrm{R})_d| \ , \tag{A4}$$

where κ is the total opacity, κ_R is the Rosseland mean opacity, and τ_R is the corresponding optical depth. We also define:

$$\Delta\tau_0 = \frac{1}{2}(\Delta\tau_- + \Delta\tau_+) \ . \tag{A5}$$

The discretized form of the equation of transfer [M78, Eq. (6-30)] is then given as:

$$\begin{aligned} &- \left(\frac{\mu_i^2}{\Delta\tau_0}\frac{1}{\Delta\tau_-}\right) u_{d-1,i} \\ &+ \left[1 + \frac{\mu_i^2}{\Delta\tau_0}\left(\frac{1}{\Delta\tau_-} + \frac{1}{\Delta\tau_+}\right)\right] u_{d,i} \\ &- \alpha_d \sum_k w_k u_{d,k} - \left(\frac{\mu_i^2}{\Delta\tau_0}\frac{1}{\Delta\tau_+}\right) u_{d+1,i} = L_{di} \ . \end{aligned} \tag{A6}$$

The thermal source terms are contained in $\boldsymbol{L}_d$:

$$L_{d\,i} = (1-\alpha_d)B(T_d) \ . \tag{A7}$$

This leads to the matrix equation [M78, Eq. (6-31)]:

$$-\boldsymbol{A}_d\boldsymbol{u}_{d-1} + \boldsymbol{B}_d\boldsymbol{u}_d - \boldsymbol{C}_d\boldsymbol{u}_{d+1} = \boldsymbol{L}_d \ . \tag{A8}$$

The diagonal components of $\boldsymbol{A}_d$, $\boldsymbol{C}_d$ and $\boldsymbol{B}_d$ are:

$$(A_d)_{ii} = \frac{\mu_i^2}{\Delta\tau_0}\frac{1}{\Delta\tau_-} \ , \tag{A9}$$

$$(C_d)_{ii} = \frac{\mu_i^2}{\Delta\tau_0}\frac{1}{\Delta\tau_+} \ , \tag{A10}$$

and

$$(B_d)_{ii} = 1 + (A_d)_{ii} + (C_d)_{ii} - \alpha_d w_i \ . \tag{A11}$$

In the original Feautrier method, the off-diagonal components of $\boldsymbol{A}_d$ and $\boldsymbol{C}_d$ are 0. The off-diagonal components of $\boldsymbol{B}_d$ are:

$$(B_d)_{ik} = -\alpha_d w_k \ . \tag{A12}$$

We solve the difference equations starting at depth because no back-substitution is needed when we are concerned with the surface flux only. With this scheme, the vector $\boldsymbol{u}_d$ is calculated from

$$\boldsymbol{u}_d = \boldsymbol{D}_d\boldsymbol{u}_{d-1} + \boldsymbol{\nu}_d \ , \tag{A13}$$

where $\boldsymbol{D}_d$ and $\boldsymbol{\nu}_d$ are defined by

$$(\boldsymbol{B}_d - \boldsymbol{C}_d\boldsymbol{D}_{d+1})\boldsymbol{D}_d = \boldsymbol{A}_d \tag{A14}$$

$$(\boldsymbol{B}_d - \boldsymbol{C}_d\boldsymbol{D}_{d+1})\boldsymbol{\nu}_d = (\boldsymbol{L}_d + \boldsymbol{C}_d\boldsymbol{\nu}_{d+1}) \tag{A15}$$

for depths $d = D-1, \ldots, 2$ (D being the lower boundary). These equations have a different form than M78, Eqs. (6-39)-(6-41), because of the reverse order of solution. Special forms of Eqs. (A6) through (A15) are required at the boundaries (see A76 and M78).

Once the solution of Eqs. (A14) and (A15) is completed, we calculate the surface flux:

$$H = \int_0^1 \mu\, u(\mu)\,\mathrm{d}\mu = \sum_{k=1}^{N} \mu_k w_k \nu_{1k} \ . \tag{A16}$$

The corresponding derivative is given by

$$\frac{\partial H}{\partial gf} = \sum_{k=1}^{N} \mu_k w_k \frac{\partial \nu_{1k}}{\partial gf} \ . \tag{A17}$$

Using the chain rule on Eqs. (A14) and (A15), we derive

$$\begin{aligned} &[\boldsymbol{B}_d - \boldsymbol{C}_d\boldsymbol{D}_{d+1}]\frac{\partial \boldsymbol{D}_d}{\partial gf} = \\ &\frac{\partial \boldsymbol{A}_d}{\partial gf} - \left[\frac{\partial \boldsymbol{B}_d}{\partial gf} - \boldsymbol{C}_d\frac{\partial \boldsymbol{D}_{d+1}}{\partial gf} - \frac{\partial \boldsymbol{C}_d}{\partial gf}\boldsymbol{D}_{d+1}\right]\boldsymbol{D}_d \end{aligned} \tag{A18}$$

and

$$\begin{aligned} &[\boldsymbol{B}_d - \boldsymbol{C}_d\boldsymbol{D}_{d+1}]\frac{\partial \boldsymbol{\nu}_d}{\partial gf} = \frac{\partial \boldsymbol{L}_d}{\partial gf} \\ &+ \boldsymbol{C}_d\frac{\partial \boldsymbol{\nu}_{d+1}}{\partial gf} + \frac{\partial \boldsymbol{C}_d}{\partial gf}\boldsymbol{\nu}_{d+1} \\ &- \left[\frac{\partial \boldsymbol{B}_d}{\partial gf} - \boldsymbol{C}_d\frac{\partial \boldsymbol{D}_{d+1}}{\partial gf} - \frac{\partial \boldsymbol{C}_d}{\partial gf}\boldsymbol{D}_{d+1}\right]\boldsymbol{\nu}_d \ . \end{aligned} \tag{A19}$$

We show the partial derivatives for the components of $\boldsymbol{A}_d$ as an example of the other matrices:

$$\frac{\partial (A_d)_{ii}}{\partial gf} = \frac{\partial (A_d)_{ii}}{\partial \Delta\tau_+}\frac{\partial \Delta\tau_+}{\partial gf} + \frac{\partial (A_d)_{ii}}{\partial \Delta\tau_-}\frac{\partial \Delta\tau_-}{\partial gf} \ , \qquad \text{(A20)}$$

where

$$\frac{\partial (A_d)_{ii}}{\partial \Delta\tau_+} = -\frac{2\mu_i^2}{\Delta\tau_-(\Delta\tau_+ + \Delta\tau_-)^2} \ , \qquad \text{(A21)}$$

$$\frac{\partial (A_d)_{ii}}{\partial \Delta\tau_-} = -\frac{2\mu_i^2(\Delta\tau_+ + 2\Delta\tau_-)}{\Delta\tau_-^2(\Delta\tau_+ + \Delta\tau_-)^2} \ , \qquad \text{(A22)}$$

and

$$\frac{\partial \Delta\tau_\pm}{\partial gf} = \frac{1}{2}\left[\left(\frac{\partial\kappa/\partial gf}{\kappa_{\rm R}}\right)_d + \left(\frac{\partial\kappa/\partial gf}{\kappa_{\rm R}}\right)_{d\pm1}\right] \times \ \left|(\tau_{\rm R})_{d\pm1} - (\tau_{\rm R})_d\right| \ . \qquad \text{(A23)}$$

Similar logic is used for the other derivatives. Note that once Eqs. (A14) and (A15) are solved at depth d, the entire right hand sides of Eqs. (A18) and (A19) are known and the solution for the partial derivatives follows. Eventually, the calculations reach the stellar surface, the boundary conditions are solved, and Eqs. (3) and (A17) are used to determine the coefficients $W_0'(\chi)$.

As shown above, in principle this method can be formulated for a scattering continuum. In the examples presented in the text, we treated scattering as ordinary absorption (without stimulated emission) because it makes little difference in the results for cool stars of solar abundance. Under this treatment, $\alpha = 0$ and all of the Feautrier matrices become diagonal; thus, the derivative matrices are also diagonal and simple multiplication and division may be used.

References

Auer L., 1976, JQSRT 16, 931, A76

Bell R.A., Tripicco M.J., 1991, AJ 102, 777

Drayson S.R., 1976, JQRST 16, 611

Hotop H., Lineberger W.C., 1985, J. Phys. Chem. Ref. Data 14, 731

Huber K.P., Herzberg G., 1979, Molecular Spectra and Molecular Structure IV. Constants of Diatomic Molecules, Van Nostrand Reinhold Company, New York

Irwin A.W., 1978, PhD Thesis, University of Toronto, Toronto, Ontario

Irwin A.W., 1981, ApJS 45, 621

Irwin A.W., 1987, A&A 182, 348

Irwin A.W., 1988, A&AS 74, 145

Jørgensen U.G., 1994a, SCAN molecular data base, J94a

Jørgensen U.G., 1994b, A&A 284, 179

Jørgensen U.G., Larsson M., 1990, A&A 238, 424

Kunasz P.B., Hummer D.G., 1974, MNRAS 166, 19

Kurucz R.L., 1991, New Opacity Calculations. In: Crivallari L., Hubeny I., Hummer D.G. (eds.) Stellar Atmospheres: Beyond Classical Models. Kluwer Academic Publishers, Netherlands, p. 441

Kurucz R.L., 1993a, Atomic Data for Opacity Calculations, CD-ROM NO. 1, K93a

Kurucz R.L., 1993b, ATLAS9 Stellar Atmosphere Programs and 2 km s^{-1} Grid, CD-ROM NO. 13

Kurucz R.L., 1993c, SYNTHE Spectrum Synthesis Programs and Line Data, CD-ROM NO. 18, K93c

Larson A.M., Irwin A.W., Yang S.L.S., Goodenough C., Walker G.A.H., Walker A.R., Bohlender D.A., 1993, PASP 105, 825

Mihalas D., 1978, Stellar Atmospheres, 2nd ed. W.H. Freeman & Company, New York, p. 151ff, M78

Martin W.C., Zalubas R., Musgrove A., 1985, J. Phys. Chem. Ref. Data 14, 751

Moore C.E., 1970, Ionization Potentials and Ionization Limits Derived from the Analyses of Optical Spectra, NSRDS – NBS 34, U.S. Government Printing Office, Washington, D.C.

Moore C.E., 1985, Selected Tables of Atomic Spectra, NSRDS – NBS 3, Section 11, U.S. Government Printing Office, Washington, D.C.

Press W.H., Teukolsky S.A., Vetterling W.T., Flannery B.P., 1992, Numerical Recipes. Cambridge University Press, Cambridge

Sauval A.J., Tatum J.B., 1984, ApJS 56, 193

Sugar J., Corliss C., 1985, J. Phys. Chem. Ref. Data 14, Suppl. 2